

# Catalytic Role of 2'-Hydroxyl Groups Within a Group II Intron Active Site

Dana L. Abramovitz, Richard A. Friedman,\* Anna Marie Pyle†

Domain 5 is an essential active-site component of group II intron ribozymes. The role of backbone substituents in D5 function was explored through synthesis of a series of derivatives containing deoxynucleotides at each position along the D5 strand. Kinetic screens revealed that eight 2'-hydroxyl groups were likely to be critical for activity of D5. Through two separate methods, including competitive inhibition and direct kinetic analysis, effects on binding and chemistry were distinguished. Depending on their function, important 2'-hydroxyl groups lie on opposite faces of the molecule, defining distinct loci for molecular recognition and catalysis by D5.

The self-splicing of group II introns is required for the expression of essential genes in many organisms (1) and may provide a simple model for catalysis by the eukaryotic spliceosome (2). The secondary structure of group II introns is typically divided into six domains, of which domain 1 (D1) and domain 5 (D5) are essential for catalysis (1). D5 is a short hairpin region of 34 nucleotides that contains most of the phylogenetically conserved nucleotides in the intron and is regarded as a central component of the group II intron active site (3). Although D5 has nanomolar binding affinity for other intronic components (4), there are no phylogenetic covariations in Watson-Crick base pairing between D5 and other regions of the intron or surrounding exons. It is therefore difficult to rationalize how D5 participates in the folding and active-site structure of group II introns. We reasoned that D5 might associate with other intronic components through tertiary contacts with its sugar-phosphate backbone, as observed in other ribozymes (5, 6).

To quantitatively assess the role of D5 2'-OH groups on reaction mechanism, we used a kinetically characterized system in which D5 catalyzes 5' splice site hydrolysis of an RNA composed of a 5' exon and domains 1 to 3 of the intron (4). This reaction has mechanistic, kinetic (4), and stereochemical (7) features similar to the first step of group II intron self-splicing. It is a useful model because D5-catalyzed hydrolysis obeys Michaelis-Menten kinetics, in which chemistry is rate-limiting and the Michaelis-Menten constant ( $K_m$ ) reflects the binding of D5 (4, 8). Given this framework for D5 activity, it was possible to make single-atom changes in D5 and kinetically determine the magnitude of effects on either binding or chemistry.

For ease of synthesis and economy, D5 molecules were synthesized as two separate strands of RNA, as if divided through the middle of the GAAA tetraloop (9). After annealing, but without covalent ligation, these strands form a D5 molecule that retains most of its original activity and binding energy (10). This result has interesting implications for the folding of the GAAA tetraloop motif (11), and it also facilitated the rapid probing of 2'-OH group requirements at every backbone position. In order to screen efficiently for D5 nucleotide positions containing critical 2'-OH groups, we synthesized chimeric D5 halves containing consecutive pairs of deoxynucleotides and examined the effects on  $k_{cat}/K_m$ . The vast majority of deoxynucleotide substitutions had no more than a twofold effect on observed rates (12). However, several chimeras showed substantially reduced activity and, for six of them, D5 activity was abolished.

In order to determine the precise locations of important 2'-OH groups, we re-synthesized those doubly substituted chimeras with greatly reduced reactivity as singly

substituted D5 derivatives. Kinetic analysis revealed six positions in which removal of a 2'-OH group eliminated D5 activity and two positions in which activity was decreased by a factor of 10 at D5 concentrations that would exceed saturation for the all-ribose molecule [wild-type (WT) D5] (4, 13). We first evaluated the basis for this diminished activity by examining the inhibition of reaction between WT D5 and its exD123 substrate. Three of the inactive chimeras, containing deoxynucleotides at positions d26, d27, and d33, competitively inhibited reaction of WT D5 (14), suggesting that they were competent for exD123 binding but unable to stimulate catalysis. The three other inactive D5 derivatives, containing deoxynucleotides at positions d8, d20, and d21, did not readily compete with WT D5, suggesting defects in binding (Table 1).

Direct measurement of kinetic behavior would provide a second means for differentiating ground- and transition-state effects of deoxynucleotide substitutions in D5. However, six of the defective chimeras had no apparent activity. To better detect any inherent reactivity in these D5 variants, we covalently joined their two halves with T4 DNA ligase (15). Ligation results in an approximate recovery of 10-fold in the  $k_{cat}/K_m$  of WT D5 molecules (with contributions from both  $k_{cat}$  and  $K_m$  effects) (10), thus widening the experimental window for examining deoxynucleotide effects. Single-deoxynucleotide chimeras that were inactive during the two-piece D5 analysis showed measurable levels of activity after ligation.

Three D5 molecules, containing deoxynucleotides at positions d26, d27, and d33, showed linear pseudo-first order kinetic behavior that readily saturated at high

**Table 1.** Effects of deoxynucleotide substitution on kinetic parameters. The kinetic parameters in columns 3 to 5 (measured as described in Fig. 1) are for ligated, one-piece D5 derivatives. Variances are standard errors obtained and validated as described previously (4). Competitive inhibition data (column 2) were obtained with two-piece D5 derivatives (14).

Deoxy-nucleotide position	Percent inhibition*	$k_{cat}/K_m$ ( $10^3 \text{ M}^{-1} \text{ min}^{-1}$ )	$k_{cat}$ ( $10^{-3} \text{ min}^{-1}$ )	$K_m$ ( $\mu\text{M}$ )	Primary effect
All-ribose WT D5	—	81 ± 16	75 ± 4.0	0.930 ± 0.13	
d8	13	7.0 ± 0.5	†	11‡	Binding
d20	6	3.6 ± 0.6	†	21‡	Binding
d21	0	5.5 ± 0.5	†	14‡	Binding
d7	§	11 ± 5.6	5.2 ± 0.6	0.49 ± 0.21	Chemistry
d26	58	6.0 ± 2.8	5.7 ± 0.7	0.94 ± 0.32	Chemistry
d27	52	9.7 ± 5.4	9.6 ± 1.4	0.99 ± 0.42	Chemistry
d29	§	8.3 ± 2.4	6.3 ± 0.5	0.75 ± 0.16	Chemistry
d33	40	3.7 ± 1.4	7.0 ± 0.9	1.2 ± 0.50	Chemistry

\*The percent inhibition of WT D5 activity under conditions where WT D5 was under  $k_{cat}/K_m$  conditions (50 nM) and the chimeric D5 was in excess, slightly greater than the WT  $K_m$  (3  $\mu\text{M}$ ) (14). †Could not be determined because of experimental limitations (see text). ‡Indicated  $K_m$  values were estimated by measuring  $k_{cat}/K_m$  from the slope of the rate data (Fig. 1B) and assuming that  $k_{cat}$  is unlikely to be substantially larger than that of WT D5 such that  $K_m(dN) = k_{cat}(WT D5) \div k_{cat}/K_m(dN)$ , where dN represents a binding-defective chimeric D5 molecule. §Values not determined because of intrinsic activity (see text).

Department of Biochemistry and Molecular Biophysics, Columbia University College of Physicians and Surgeons, New York, NY 10032, USA.

\*Present address: Computer Facility of the Columbia Presbyterian Cancer Center, New York, NY 10032, USA. †To whom correspondence should be addressed.

concentrations of D5 (Fig. 1A and Table 1) (16). The resultant  $K_m$  values for these molecules were indistinguishable from that of WT D5, indicating that the binding strength of these chimeras was unaffected, and there was unlikely to be a change in rate-limiting step or the introduction of conformational perturbations (17). However,  $k_{cat}$  values (rates at total saturation) were reduced by a factor of at least 10. Therefore, consistent with the competitive inhibition data, these chimeras are competent for binding the other reaction components, and their primary defect is likely to occur during the chemical step. This result implies that 2'-OH groups at positions d26, d27, and d33 have a function in the transition state but not the ground state. Although direct effects on catalysis represent the simplest interpretation of the data, it is possible that the chemical effects result from subtle structural changes that perturb only the transition state. This interpretation is particularly reasonable for ribose

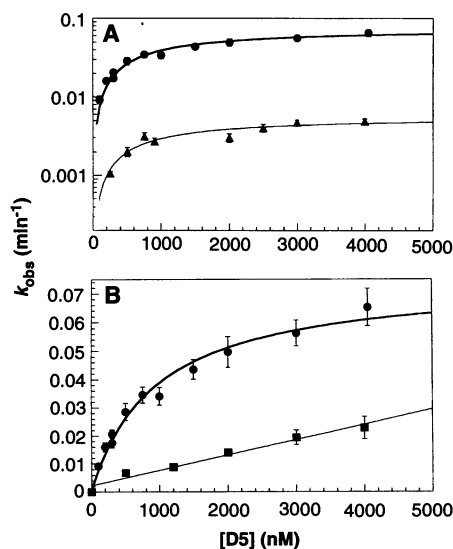


**Fig. 1.** Kinetic behavior of deoxynucleotide-substituted D5 derivatives. Rate versus D5 concentration plots (Michaelis-Menten binding curves) are shown. Rates ( $k_{obs}$ ) were determined under single-turnover conditions from pseudo-first order plots and quantitated as described for WT D5 (4). Error bars describe the variance in pseudo-first order rate data. (A) Comparison of WT D5 (●) to chemically defective d26 (▲). For these D5 derivatives and the chemically defective chimeras d7, d27, d29, and d33, plots of  $k_{obs}$  versus [D5 derivative] fit a standard binding equation (4). Values for  $K_m$  and  $k_{cat}$  were derived from fits of the data to this equation and are provided in Table 1. The logarithm of  $k_{obs}$  is plotted here so that both sets of data fit on the same scale. (B) Comparison of WT D5 (●) to the binding-defective d21 (■). In this instance, all values for  $k_{obs}$  are plotted on a standard linear scale, and the raw data for WT D5 are the same as in (A). For the binding-defective derivatives d8 and d20, plots of  $k_{obs}$  versus [D5] were linear as shown in this example for d21.

d33, which is diagonally adjacent to a nucleobase essential for chemistry.

Conversely, D5 derivatives containing deoxynucleotides at positions d8, d20, and d21 showed strong ground-state binding defects. Unlike the WT D5 (4), reactivity of these chimeras did not plateau or show saturation behavior (Fig. 1B and Table 1). Instead, there was a linear increase in rate with increasing D5 concentration, typical of the early region in a binding curve below  $K_m$ . That the chemical reactivity of these chimeras remained largely intact is suggested by the fact that their maximum rates are actually rather fast, being comparable to those of WT D5 at concentrations just below its  $K_m$  (Fig. 1B). The apparent binding defects in these chimeras are consistent with their failure to competitively inhibit WT D5 (Table 1). Although they contribute a large amount of binding energy ( $-5.2$  kcal/mol), 2'-OH groups at d8, d20, and d21 cannot account for all of the D5 binding affinity ( $-8.7$  kcal/mol), which is likely to include additional contributions from nucleobase and phosphate contacts (17).

Two of the chimeric species, containing deoxynucleotides at positions d7 and d29, had effects on both binding and chemistry (Table 1). The largest effects were on  $k_{cat}$ , but effects on  $K_m$  were also evident. In this instance, it is difficult to confidently ascribe the  $k_{cat}$  effects solely to chemistry because the decrease in  $K_m$  may be indicative of alternative conformations or nonproductive binding (18). In addition, there are no competitive inhibition data for comparison because these two chimeras, in their unligated form, had low levels of reactivity that inherently complicated indirect competitive analysis. Whereas binding of these species may simply be tighter, data for these D5 derivatives may reflect additional kinetic events.

The same major effects on function were observed with two different experimental methods: competitive inhibition and single-turnover kinetic analysis (Table 1). In addition, chimeric oligonucleotides containing a particular deoxynucleotide substitution were synthesized at least twice. All of these experiments were done within a kinetic framework that itself was validated through numerous procedures (8). Therefore, we propose that at least three 2'-OH groups, at positions d26, d27, and d33, are involved in the chemical step of reaction and that three 2'-OH groups are involved in binding between D5 and intronic components such as D1. With this result established, it is informative to examine the spatial relations among these 2'-OH groups on a two-dimensional representation of D5 (Fig. 2). There are three regions in which the critical 2'-OH groups cluster: adjacent to the invariant AGC catalytic triad in

helix 1; flanking the two-nucleotide bulge between the helices; and in the GAAA tetraloop.

Of these clustered regions, the least surprising effects are those at d20 and d21, in the tetraloop. Crystallographic analysis of packing interactions by the hammerhead ribozyme showed that GAAA loop nucleotides 3 and 4 dock into the minor groove of two tandem G-C pairs on an adjacent RNA helix (17). The 2'-OH groups on loop nucleotides 3 and 4 are involved in hydrogen bonds that appear to stabilize this tertiary interaction. Evidence that these groups contribute energetic stabilization to such an interaction is actually provided by the data herein. The docked-tetraloop motif is important in the folding of group I introns (19), and in group II introns the GAAA tetraloop of D5 was recently proposed to interact with a particular region of domain 1 (20). Whereas our data support an interaction of this type, the exact location of docking is complicated by the fact that several sets of tandem G-C pairs in ai5g D1 can potentially contact the tetraloop. For the WT ai5g intron sequence, such as that studied here, the putative docking site contains inverted G-C pairs (a G-C followed by a C-G), rather than the tandem purine-pyrimidine pairs observed to form characteristic hydrogen bonding arrays with GNRA tetraloops (17, 19).

Invariant bases G6 and C7 have been shown to be directly involved in the chemical step of reaction (21). Therefore, it is reasonable that one or more 2'-OH groups in this region will also participate in chemistry. Chimeras containing 2'-OH groups at positions d7, d8, and d33 are adjacent or attached to the phylogenetically invariant AGC residues at positions 5, 6, and 7 (Fig. 2). In addition, several important 2'-OH

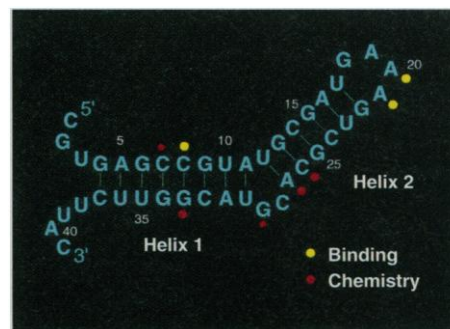


**Fig. 2.** Positions of critical 2'-OH groups on D5. Nucleotide positions where deoxyribose substitution results in a greater than 10-fold effect on binding (yellow,  $K_m$ ) or chemistry (red,  $k_{cat}$ ) are indicated. The large balls indicate positions where kinetic effects can be clearly ascribed to a particular type of defect (binding or chemistry). Smaller balls represent ribose positions with kinetic effects that are more complex and less easily assigned strictly to binding or chemistry.

groups in this region are immediately adjacent to the G-U wobble pair involving G6 and U35. G-U wobble pairs often occur next to clusters of critical 2'-OH groups, as seen in tRNA<sup>Ala</sup> and the *Tetrahymena* ribozyme (22).

While the biochemical work was in progress, we independently developed a three-dimensional model of D5, using the RNA modeling program MC-SYM (23) together with coordinates from the crystallographically determined GAAA tetraloop structure (17). Construction of the model was followed by minimization with Discover (Fig. 3). The accessibilities and base pairing patterns for nucleotides 3 to 38 of the model are consistent with results from chemical modification studies on D5 (24, 25). Important 2'-OH groups were superimposed onto this model along with nucleobases (21) and phosphate oxygen residues (25) implicated in D5 reactivity (Fig. 3, A and B). Despite the fact that these different residues were identified independently in three separate laboratories by different methods, the correlation between function and spatial position on the molecule is in remarkable agreement.

There appear to be two distinct faces of D5—a binding face (Fig. 3A) and a chemical face (Fig. 3B)—such that D5 is sandwiched directly between intronic components involved in ground-state docking and chemical reactivity. The positions of 2'-OH groups in-

volved in binding span a full turn of the helix (Fig. 3A, yellow). Thus, the tetraloop and lower portions of D5 are each important for ground-state association with a spatially contiguous recognition surface. By positioning the ground-state interactions along one side of D5, the other side of the helix is made available for participation in the transition state through a set of distinct chemical functionalities (Fig. 3B, red and pink). The backbone functionalities important for chemistry surround both sides of the major groove, in spatial proximity to the catalytically essential G6 and C7 nucleobases. This localization of D5 chemical functionalities suggests a possible alignment with the 5' splice site, which can be visualized as a continuous duplex containing a two-nucleotide gap between the intron binding site 1–exon binding site 1 (IBS1–EBS1) and  $\epsilon$ - $\epsilon'$  helices (1). The single-stranded gap containing the cleavage site may align over the catalytic region of D5, and the adjacent helices provide a context for marking the scissile phosphate for specific cleavage by functionalities on D5 and elsewhere in the intron. This concept is more credible if one assumes that, in the bound form, the major groove at the chemical active site is wider than predicted by our ground-state model, thus rendering the G6 and C7 nucleobases more accessible.

One can envision a number of chemical roles for 2'-OH groups in the transition state. In a recent hypothetical model, it was pro-

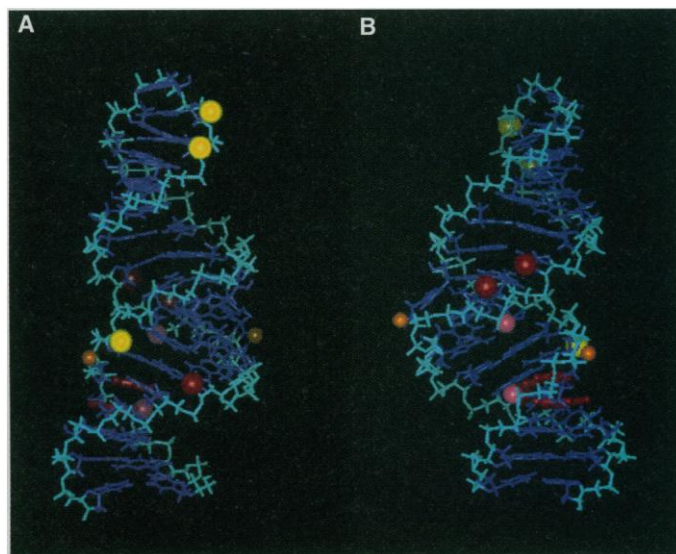
posed that D5 is a two-metal binding platform in the group II intron active site (26). Our model places the two essential phosphates [neither of which has been implicated in metal binding (25)], along with 2'-OH groups and other potential metal ligands, in a spatial arrangement that could accommodate a two-metal mechanism. However, there is insufficient information to assign a role in metal binding to any of these groups. Although 2'-OH oxygens are not generally described as strong metal ligands, they are reasonable outer sphere ligands for metal-aquo species, and their affinity for direct metal binding may actually increase within the altered chemical environment of the ribozyme core. The core medium may have other effects on reactivity, including changes in  $pK_a$  that help 2'-OH groups stabilize the nucleophile or the leaving group in the transition state. Alternatively, the cluster of chemically essential backbone atoms may play a role in water or hydroxide organization, contributing a network of bonds that lower the activation barrier for reaction.

Previous work indicates that 2'-OH functionalities readily participate in important ground-state interactions, stabilizing the binding or folding of RNA structures (5, 6). Chemical roles have been primarily ascribed to the 2'-OH at scissile phosphodiester linkages (27). As a consequence, we expected to find that the 2'-OH groups of D5 would function as ground-state recognition elements, rather than chemically significant components of an enzyme-active site. We show that 2'-OH groups on a ribozyme may coalesce into catalytically reactive sites, lowering the transition state stabilization energy for oligonucleotide cleavage. The behavior of D5 shows that there may be a division of labor among 2'-OH groups and that, on the same molecule, some of them will mediate binding, whereas others affect chemical reactivity. Thus, the multifunctional nature of this group imparts a versatility that extends from binding to catalysis.

## REFERENCES AND NOTES

1. F. Michel and J.-L. Ferat, *Annu. Rev. Biochem.* **64**, 435 (1995); A. M. Pyle, *Nucleic Acids Mol. Biol.*, in press.
2. Y.-T. Yu, P. A. Maroney, E. Darzynkiewicz, T. W. Nilsen, *RNA* **1**, 46 (1995); H. D. Madhani and C. Guthrie, *Cell* **71**, 803 (1992); T. R. Cech, *ibid.* **44**, 207 (1986).
3. K. A. Jarrell, R. C. Dietrich, P. S. Perlman, *Mol. Cell. Biol.* **8**, 2361 (1988); J. L. Koch, S. C. Boulanger, S. D. Dib-Hajj, S. K. Hebbbar, P. S. Perlman, *ibid.* **12**, 1950 (1992); S. C. Boulanger *et al.*, *ibid.* **15**, 4479 (1995).
4. A. M. Pyle and J. B. Green, *Biochemistry* **33**, 2716 (1994); J. S. Franzen, M. Zhang, C. L. Peebles, *Nucleic Acids Res.* **21**, 627 (1993); D. L. Daniels, W. J. Michels, A. M. Pyle, *J. Mol. Biol.* **256**, 31 (1996).
5. A. M. Pyle and T. R. Cech, *Nature* **350**, 628 (1991); A. M. Pyle, F. L. Murphy, T. R. Cech, *ibid.* **358**, 123 (1992); S. A. Strobel and T. R. Cech, *Biochemistry* **32**, 13593 (1993); D. Herschlag, F. Eckstein, T. R.

**Fig. 3.** Three-dimensional organization of important D5 functional groups. Important ribose, phosphate, and nucleobase functionalities are placed upon a hypothetical model for the structure of unbound D5. The binding face (A) and the chemical face of D5 (B) are two different views of the same structure. 2'-Hydroxyl groups important for binding (yellow) cluster on the binding face (A), whereas 2'-OH groups and other functionalities important for chemistry (red) cluster on the chemical face (B). Nucleobases G6 and C7 have been shown to affect chemistry (21) and are therefore shown in red. Shown in pink are the two Rp phosphate oxygens that, when substituted with sulfur atoms, result in a complete block of splicing at high salt concentrations (25). Orange balls indicate important 2'-OH groups that have a mixture of effects, potentially due to flexibility in positioning (in the case of d29, left) or direct attachment to a chemically important nucleobase (in the case of d7, right). The model was generated as described in the text (Discover, version 2.9; Biosym Technologies, San Diego, California, 1992). It was minimized with Amber potential parameters and a constant dielectric of 120 (28). The model is a typical A-form RNA helix with proper sugar puckering and base pairing. The cytidine of the internal loop is stacked into the helix, whereas the sterically larger G is out of the helix, consistent with chemical modification patterns of unbound D5 (25). The nucleotides shown in this three-dimensional model begin at residues U3 and end at U38, according to the numbering scheme shown in Fig. 2.



- Cech, *ibid.*, p. 8299.
- P. C. Bevilacqua and D. H. Turner, *Biochemistry* **30**, 10632 (1991).
  - M. Podar, P. S. Perlman, R. A. Padgett, *Mol. Cell Biol.* **15**, 4466 (1995).
  - That  $k_{\text{cat}} = k_{\text{chem}}$  and  $K_m = K_d$  in this reaction is supported by the fact that single- and multiple-turnover analyses of the reaction yield the same kinetic parameters (4); the value for  $K_m = K_d$  determined through direct measurements (4);  $k_{\text{cat}}$  varies logarithmically with pH (4); and phosphorothioate substitution results in apparent rate effects of a magnitude typical for chemically limited reactions (7).
  - The 41-nt D5, containing seven flanking nucleotides, was synthesized in two pieces on an ABI 392 DNA/RNA synthesizer and worked up according to standard procedures [S. A. Scaringe, C. Francklyn, N. Usman, *Nucleic Acids Res.* **18**, 5433 (1990)]. Oligonucleotides were purified on a Waters high-performance liquid chromatography (HPLC) system with a Machery-Nagel Nucleogen DEAE 60-7 column. Oligonucleotides were then desalted with ABI Oligonucleotide Purification Cartridges following the manufacturer's instructions.
  - $K_m = 1.5 \pm 0.6 \mu\text{M}$ ,  $k_{\text{cat}} = 0.02 \pm 0.002 \text{ min}^{-1}$ , and  $k_{\text{cat}}/K_m = 1.3 \times 10^4 \text{ M}^{-1} \text{ min}^{-1}$ . Parameters were determined under reaction conditions of 100 mM  $\text{MgCl}_2$ , 500 mM KCl, and 40 mM MOPS (pH 7.5) at 45°C as described (4).
  - D. L. Abramovitz and A. M. Pyle, in preparation.
  - In predominantly RNA duplexes, a single deoxyribonucleotide is expected to exist primarily in the C3'-endo conformation of its neighbors, resulting in minimal perturbations of the structure. Although twofold effects on binding constants of oligonucleotide strands have been observed (6), these would be invisible here because each D5 chimera was preincubated before reaction to ensure full annealing of the strands. Aside from effects on D5 duplex stability, single deoxynucleotides may affect electrostatics and local water structure. However, if water organization is important to catalytic activity and such activity is mediated by a 2'-OH group, we consider such effects to represent important contributions to the catalytic process.
  - Effects smaller than 10-fold were observed for several of the deoxynucleotide-substituted D5 derivatives. Description of these smaller effects is detailed in (11).
  - Competitive inhibition was evaluated under  $k_{\text{cat}}/K_m$  conditions for WT D5 (50 nM D5, 1 nM  $^{32}\text{P}$ -exD123), which are the most sensitive for measurement of competitor effects [J. A. Doudna and T. R. Cech, *RNA* **1**, 36 (1995)]. WT D5 was in one piece, whereas competitor chimeric D5 molecules were provided in excess as two-piece annealed strands (3  $\mu\text{M}$ ). Competitor D5 derivatives containing both single- and double-deoxynucleotide substitutions were tested, and for substitutions at similar positions the same results were obtained. Kinetics were measured under standard conditions (10).
  - M. J. Moore and P. A. Sharp, *Science* **256**, 992 (1992).
  - There were no lags during initial portions of the the first-order plots, which were linear for all chimeras described in this study (data not shown).
  - H. M. Pley, K. M. Flaherty, D. B. McKay, *Nature* **372**, 111 (1994).
  - In these single-turnover experiments, changes in rate are likely to involve only the following parameters:  $k_{\text{on}}$  or  $k_{\text{off}}$  of substrate;  $k_{\text{chem}}$ , a rate-limiting conformational change within the E·S complex (equivalent to an intermediate occurring after E·S); or nonproductive binding of substrate. The lack of perturbations in  $K_m$  argue against all of the above possibilities with the exception of a change in  $k_{\text{chem}}$  because  $K_m = k_{\text{off}}/k_{\text{on}}$ , so it would directly reflect a change in  $k_{\text{off}}$  or  $k_{\text{on}}$ . A Michaelis-Menten mechanism stipulates that  $k_{\text{chem}}$  is slower than  $k_{\text{on}}$  or  $k_{\text{off}}$ , so a reduction in  $k_{\text{chem}}$  does not alter the mechanism. The introduction of a rate-limiting conformational change is equivalent to the formation of intermediates after E·S, and nonproductive binding introduces additional equilibrium constants—both of which result in a  $K_m$  that appears artificially tighter [ $K_m < K_d$ ; A. Fersht, *Enzyme Structure and Mechanism* (Freeman, New York, 1985), pp. 102–109].
  - L. Jaeger, F. Michel, E. Westhof, *J. Mol. Biol.* **236**, 1271 (1994); L. Jaeger, E. Westhof, F. Michel, *ibid.* **236**, 331 (1993); F. L. Murphy and T. R. Cech, *ibid.* **236**, 49 (1994); A. M. Pyle and J. B. Green, *Curr. Opin. Struct. Biol.* **5**, 303 (1995).
  - M. Costa and F. Michel, *EMBO J.* **14**, 1276 (1995).
  - C. L. Peebles, M. Zhang, P. S. Perlman, J. F. Franzen, *Proc. Natl. Acad. Sci. U.S.A.* **92**, 4422 (1995).
  - K. Musier-Forsyth and P. Schimmel, *Nature* **357**, 513 (1992); A. M. Pyle *et al.*, *Biochemistry* **33**, 13856 (1994); D. S. Knitt, G. J. Narlikar, D. Herschlag, *ibid.*, p. 13864; S. A. Strobel and T. R. Cech, *Science* **267**, 675 (1995).
  - F. Major *et al.*, *Science* **253**, 1255 (1991).
  - J. H. Kwakman, D. A. Konings, P. Hogeweg, H. J. Pel, L. A. Grivell, *J. Biomol. Struct. Dyn.* **8**, 413 (1990).
  - G. Chanfreau and A. Jacquier, *Science* **266**, 1383 (1994).
  - T. A. Steitz and J. A. Steitz, *Proc. Natl. Acad. Sci. U.S.A.* **90**, 6498 (1993).
  - D. Herschlag, F. Eckstein, T. R. Cech, *Biochemistry* **32**, 8312 (1993); D. Smith and N. R. Pace, *ibid.*, p. 5273.
  - S. J. Weiner, P. A. Kollman, D. T. Nguyen, D. A. Case, *J. Comp. Chem.* **7**, 230 (1986); R. A. Friedman and B. Honig, *Biopolymers* **32**, 145 (1992).
  - We thank B. Honig and M. Akke for helpful discussion of the D5 model, S. Strobel for discussion of the data and help with ligations, and Z. Qin and B. Konforti for critical review of the manuscript. We also thank F. Major for use of, and help with, MC-SYM; D. McKay for the coordinates of the GAAA tetraloop in the hammerhead ribozyme; and C. Bingman for advice on HPLC. Supported by grants GM50313 to A.M.P. and GM41371 to B. Honig from the National Institutes of Health.

16 October 1995; accepted 11 January 1996

## Uncoupling of GTP Binding from Target Stimulation by a Single Mutation in the Transducin $\alpha$ Subunit

Rohit Mittal, Jon W. Erickson, Richard A. Cerione\*

Glutamic acid-203 of the alpha subunit of transducin ( $\alpha_T$ ) resides within a domain that undergoes a guanosine triphosphate (GTP)-induced conformational change that is essential for effector recognition. Changing the glutamic acid to an alanine in bovine  $\alpha_T$  yielded an alpha subunit ( $\alpha_T$ E203A) that was fully dependent on rhodopsin for GTP-guanosine diphosphate (GDP) exchange and showed GTP hydrolytic activity similar to that measured for wild-type  $\alpha_T$ . However, unlike the wild-type protein, the GDP-bound form of  $\alpha_T$ E203A was constitutively active toward the effector of transducin, the cyclic guanosine monophosphate phosphodiesterase. Thus, the  $\alpha_T$ E203A mutant represents a short-circuited protein switch that no longer requires GTP for the activation of the effector target phosphodiesterase.

Heterotrimeric GTP-binding proteins (G proteins) serve as molecular switches in various receptor-coupled signal transduction pathways including those responsible for hormone-regulated adenyl cyclase activity, receptor-stimulated phosphoinositide lipid turnover, ion channel regulation, ol-

faction, taste, and vertebrate vision (1, 2). The phototransduction cascade in which rhodopsin activates the G protein transducin has frequently been used as a paradigm for receptor signaling mediated by G proteins. The three-dimensional structures of  $\alpha_T$  bound to GDP and  $\alpha_T$  bound to guanosine 5'-O-(3-thiotriphosphate) (GTP- $\gamma$ -S), as well as the aluminum fluoride ( $\text{AlF}_4^-$ )-activated  $\alpha_T$  subunit, have been solved (3–5). This structural information

provides a foundation for understanding the molecular basis by which rhodopsin-stimulated GTP binding to transducin converts this molecule into an activated transducer that directs the regulation of a specific effector protein.

Direct comparisons of the tertiary structures of the GDP-bound and GTP- $\gamma$ -S-bound  $\alpha_T$  subunits indicate that there are three regions that undergo changes in tertiary conformation as an outcome of GTP-GDP exchange (4). Two of these regions, designated as switch I (Ser<sup>173</sup> to Thr<sup>183</sup> in  $\alpha_T$ ) and switch II (Phe<sup>195</sup> to Thr<sup>215</sup> in  $\alpha_T$ ), are analogous to conformationally sensitive regions found in the Ras and EF-Tu proteins, whereas a third region, designated switch III (Asp<sup>227</sup> to Arg<sup>238</sup> in  $\alpha_T$ ), may undergo structural changes that are specific to heterotrimeric G proteins (4). The switch II region is especially important because it serves as a critical interface, mediating the changes induced within the switch I region by GTP binding into effector recognition. Thus, individual residues within the switch II domain have served as indicators for G protein activation; two examples being Arg<sup>204</sup> of the  $\alpha_T$  subunit, which is no longer sensitive to trypsin when  $\alpha_T$  is in the GTP-bound (or  $\text{AlF}_4^-$ -bound) state, and Trp<sup>207</sup> of  $\alpha_T$ , which shows an enhanced fluorescence when activating li-

Department of Pharmacology, Cornell University, Ithaca, NY 14853–6401, USA.

\*To whom correspondence should be addressed.